Techno-Economic and Life Cycle Analysis of Synthetic Methanol Production from Hydrogen and Industry By-product CO_2

Guiyan Zang, Pingping Sun, Amgad Elgowainy, and Michael Wang*

Systems Assessment Center, Energy Systems Division, Argonne National Laboratory, 9700 South Cass Avenue, Lemont, Illinois 60439, United States

KEYWORDS

Synthetic methanol; Techno-economic analysis; Life cycle analysis; GHG emissions; High-purity CO_2 sources; E-fuels; CO_2 utilization

ABSTRACT

CO_2 capture and utilization provides an alternative pathway for low-carbon hydrocarbon production. Given the ample supply of high purity CO_2 emitted from ethanol and ammonia plants, this study conducted techno-economic analysis and environmental life cycle analysis of several systems: integrated methanol-ethanol co-production, integrated methanol-ammonia co-production, and stand-alone methanol production systems, using CO_2 feedstock from ethanol plants, ammonia plants, and general market CO_2 supply. The cradle-to-grave greenhouse gas emissions of methanol produced from the stand-alone methanol, integrated methanol-ethanol, and integrated methanol-ammonia systems are 13.6, 37.9, and 84.6 g CO_2-eq./MJ, respectively, compared to 91.5 g CO_2-eq./MJ of conventional methanol produced from natural gas. The minimum fuel selling price (MFSP) of methanol ($0.61–0.64/kg) is 61–68% higher than the average market methanol price of $0.38/kg, when using a Department of Energy target renewable

hydrogen production price of $2.0/kg. The methanol price increases to $1.24–1.28/kg when the hydrogen price is $5.0/kg. Without CO_2 abatement credits, the H_2 price needs to be within $0.77–0.95/kg for the MFSP of methanol to equal the average methanol market price. With a CO_2 credit of $35/MT according to tax credit per metric ton of CO_2 captured and used, the methanol price is reduced to $0.56–0.59/kg.

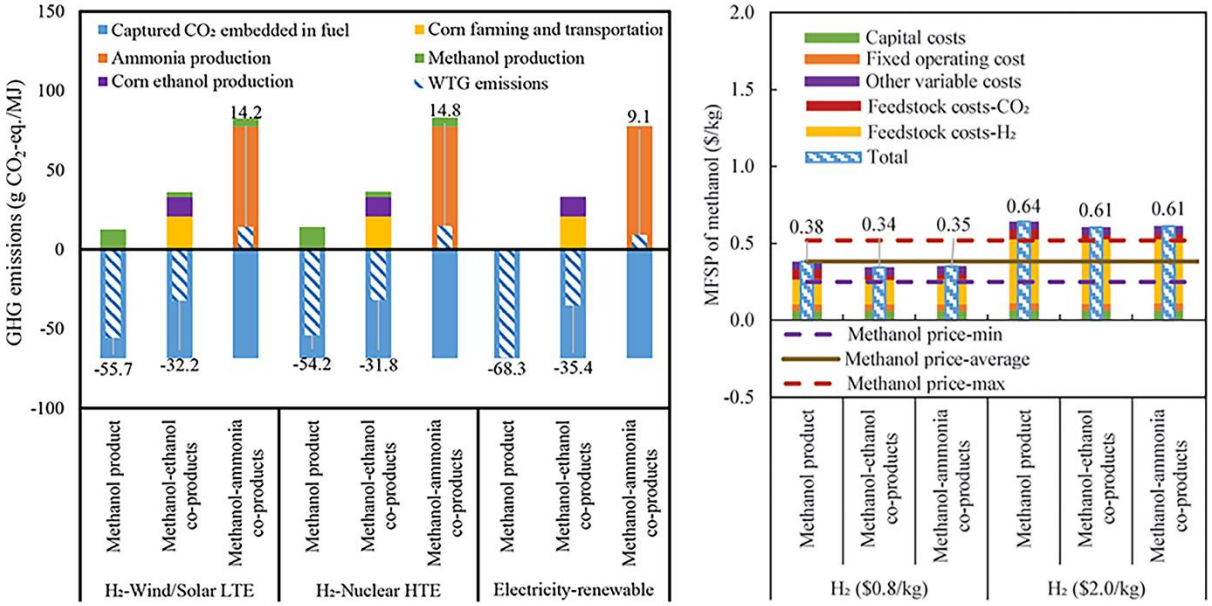

SYNOPSIS

This study evaluated GHG emissions and the cost of methanol produced from industrial waste CO_2 with a comprehensive sensitivity analysis.

INTRODUCTION

The transportation and industry sectors accounted for 36% and 26% of U.S. carbon dioxide (CO_2) emissions from fossil fuel combustion in 2018, respectively, including both direct fossil fuel use and electricity use.[1] Given that CO_2 emission is the main driver for global warming, there has been

increased interest in replacing fossil fuels in these sectors by accelerating the deployment of low-carbon fuels.[2,3] CO_2 capture and utilization (CCU) provides opportunities to synthesize low-carbon hydrocarbon fuels and chemicals by using captured CO_2 as the feedstock and zero-carbon electricity or renewable hydrogen as the energy source.[4] CCU essentially extends the life of CO_2 over another fuel or chemical product cycle.[5] Thus, CCU for fuel production can reduce consumption of fossil sources and the resultant emissions.[6]

Although the industrial sector emitted 970 MMT (million metric ton) of CO_2 in 2018,[1] the CO_2 capture from the industrial sector is limited to about 1% of total industrially produced CO_2.[7] The CO_2 emissions from industrial sources can be distinguished as combustion emissions (occurring from fuel combustion) and process emissions (e.g., due to non-combustion chemical reactions).[8] Some process emissions from biochemical or chemical reactions, for example, CO_2 emissions from ethanol fermentation and amine separation, have a purity higher than 97%.[9] With about 44 MMT and 19 MMT CO_2 emissions from ethanol plants (fermentation) and ammonia plants (amine separation) each year, the high-purity CO_2 supply in the United States is abundant.[7,10] Given that the higher-purity CO_2 emissions translate into lower capture costs,[11] the present study uses high purity CO_2 from ethanol and ammonia plants as the feedstock for CCU.

Electro-fuels (e-fuels) or synthetic hydrocarbons production from water and waste CO_2 streams, with zero-carbon electricity as the primary energy source, are of increasing interest recently.[12] Among various production routes, synthetic methanol has been extensively researched due to its potential as a low-carbon fuel, energy carrier, or fuel blending component, and the relative ease of its production.[13] Low- or zero-carbon electricity is used as an energy source to split water and produce hydrogen (H_2) for methanol product in a one-step (directly) or two-step process.[14] The one-step process produces methanol from CO_2 and H_2 directly,[13] while the two-step process

converts CO_2 to CO through a reverse water gas shift (RWGS) reaction, and then hydrogenates CO with H_2 to form methanol.[15] Relative to the one-step pathway, the two-step pathway has a higher methanol yield per pass, lower catalyst cost, and smaller hydrogenation reactor size.[16] Thus, this study focuses on the techno-economic analysis (TEA) and life cycle analysis (LCA) of the two-step pathway of e-fuel methanol synthesis.

Previous TEA analysis results showed that the minimum fuel selling price (MFSP) of synthetic methanol produced from waste CO_2 and H_2 using wind or solar electricity is $1.00–1.50/kg, more than two times higher than the market methanol price of around $0.45/kg.[15,17–20] However, the synthetic methanol pathway can provide significant greenhouse gas (GHG) emissions reduction benefit. For example, previous studies showed that synthetic methanol can be produced from waste CO_2 using H_2 from water electrolysis. When the H_2 is produced via electrolysis using renewable electricity, the cradle-to-gate (CTG) GHG emissions of the synthetic methanol are lower than -49.7 g CO_2-eq./MJ.[15,17–21] Thus, compared to the CTG GHG emissions of 23.7 g CO_2-eq./MJ for conventional methanol production from natural gas (does not include methanol combustion CO_2 emissions), the synthetic methanol produced from waste stream CO_2 and renewable electricity is a low-carbon production pathway.[22]

Although previous studies evaluated the LCA and/or TEA of e-fuel (synthetic) methanol production in different regions and from various sources, the synthetic methanol production utilizing high purity CO_2 waste from ethanol and ammonia plants in the United States, considering expanded system boundary and various hydrogen pathways, has not been thoroughly evaluated. To fill this gap, the LCA and TEA of this study used three CO_2 waste sources from ethanol plants (process CO_2 from fermentation), ammonia plants (with amine scrubbing), and general market CO_2 supply.

Three CO_2 collecting costs of $17.3/MT (metric ton), $20.6/MT, and $38.6/MT for high purity CO_2 from the ethanol plant, the ammonia plant, and market supply were used for the TEA.[23] The LCA of synthetic methanol production was evaluated by defining three system boundaries: integrated methanol-ethanol co-production system boundary, integrated methanol-ammonia co-production system boundary, and stand-alone methanol production system boundary. For the LCA and TEA, the synthetic methanol was produced from renewable H_2 (via water electrolysis) and high purity CO_2, through the two-step reaction process, which was simulated using the Aspen Plus model. The LCA was conducted using the GREET® (Greenhouse gases, Regulated Emissions and Energy use in Technologies) 2020 model, whereas the TEA leveraged the H2A model framework.[24] Both of the CTG and cradle-to-grave GHG emissions of the synthetic methanol were evaluated for various H_2 pathways, and electricity types. The sensitivity of methanol MFSP to a wide range of H_2 prices and potential CO_2 credits was evaluated.

METHODOLOGY

Synthetic Methanol Production Overview

Using various CO_2 supply options, the present study focused on three systems: methanol-ethanol co-production, methanol-ammonia co-production, and stand-alone methanol production, as shown in Figure 1. GREET® includes detailed mass, emissions, and energy inventory information for ethanol production (dry milling corn ethanol process with corn oil extraction), ammonia production, and H_2 production. Aspen Plus software was used to simulate the methanol produced from H_2 and CO_2, which provided mass and energy balance and flow information for LCA and TEA. Methanol is produced from H_2 and CO_2 through a two-step pathway: H_2 reacts with CO_2 to

produce CO through an RWGS reaction, denoted as (R1);[25] and CO/CO_2 react with H_2 to generate methanol through synthesis reactions, denoted as (R2) and (R3).[26]

$$CO_2 + H_2 \leftrightarrow CO + H_2O \qquad \Delta H^0 = +41\ kJ/mol \qquad \text{(R1)}$$

$$CO_2 + 3H_2 \leftrightarrow CH_3OH + H_2O \qquad \Delta H^0 = -87\ kJ/mol \qquad \text{(R2)}$$

$$CO + 2H_2 \leftrightarrow CH_3OH \qquad \Delta H^0 = -128\ kJ/mol \qquad \text{(R3)}$$

RWGS (R1) is endothermic, which requires a high reaction temperature for a reasonable conversion and needs heat supply. Both (R2) and (R3) are exothermic reactions that alleviate the total process of energy demand.

The methanol production process is modeled in five reaction areas (see Figure 1), while the detailed technical parameters are provided in Table S1 (Supporting Information). In area A1, H_2 and CO_2 are compressed to 2.47 MPa.[27,28] In A2, compressed H_2 and CO_2, with 1:1 molar ratio, react in the RWGS reactor at 600 °C and 2.45 MPa to convert 36% of CO_2 into CO.[29] A Selexol CO_2 capture unit (A2) is utilized to remove CO_2 and increase the CO molar concentration in the syngas from 31% to 60%.[30] The RWGS reaction is based on the experimental result of Kim et al. (2014) using $BaCe_{0.2}Zr_{0.6}Y_{0.16}Zn_{0.04}O_3$ as the catalyst.[29] In reaction area 3 (A3), H_2 and CO gases, with 2.1:1 molar ratio, flow through the reactor to synthesize methanol via chemical equilibrium reactions. The methanol reactor has a CO conversion ratio of 17% per pass at 300 °C and 5.1 MPa.[31] Three reactors in series are used in the Aspen model, with 89% of the effluent gas recycled to the methanol reactors (flue gas recycle in Figure 1), around 90% of the total CO is converted into methanol. After the effluent gas recycle, 85% of the H_2 is separated by pressure swing adsorption (PSA) and recycled to the H_2 compressor.[32] Finally, methanol is distilled and cooled for product storage, while all the combustible components from A3 are fed to the boiler for

combustion to provide heat at 900 °C for the RWGS reactor (A4).[33] The last reaction area (A5) accounts for the energy and water balance of the total system, including cooling towers, material storage, and wastewater treatment units. The cooling tower operates at temperatures between 28 °C and 37 °C with a cooling water recycling efficiency of 99.85%.[34]

For the stand-alone system, the methanol production efficiency, cold gas efficiency, and the carbon conversion efficiency are defined by Equations (1), (2) and (3), respectively. For all three system boundaries considered in this analysis, the CTG methanol energy efficiency and CTG total energy efficiency are derived from Equations (4) and (5), respectively.[35,36]

$$\eta_{E,M} = E_M/(E_{H_2} + W_E) \quad (1)$$

$$\eta_{E,CM} = E_M/(E_{H_2}) \quad (2)$$

$$\eta_{C,M} = (C_M)/C_{CO_2} \quad (3)$$

$$\eta_{E,M,CTG} = E_M/(E_{RE,CTG} + W_{FE,CTG}) \quad (4)$$

$$\eta_{E,T,CTG} = (E_M + E_O)/(E_{RE,CTG} + W_{FE,CTG}) \quad (5)$$

Where, $\eta_{E,M}$, $\eta_{E,CM}$, $\eta_{E,M,CTG}$, $\eta_{E,T,CTG}$, and $\eta_{C,M}$ are the methanol production efficiency from H_2 and CO_2; methanol production cold gas efficiency, CTG methanol energy efficiency, CTG total energy efficiency (including energy in co-products), and methanol carbon conversion efficiency from CO_2, respectively. E_M is the energy of methanol, E_O is the energy of other co-products; E_{H_2} and W_E are the H_2 energy and electricity input to the methanol production process from H_2 and CO_2; $E_{RE,CTG}$ is the CTG renewable energy input, and $W_{FE,CTG}$ is the CTG fossil energy input. C_M and C_{CO_2} are the carbon content in methanol and high purity CO_2 input for the stand-alone methanol produced from H_2 and CO_2.

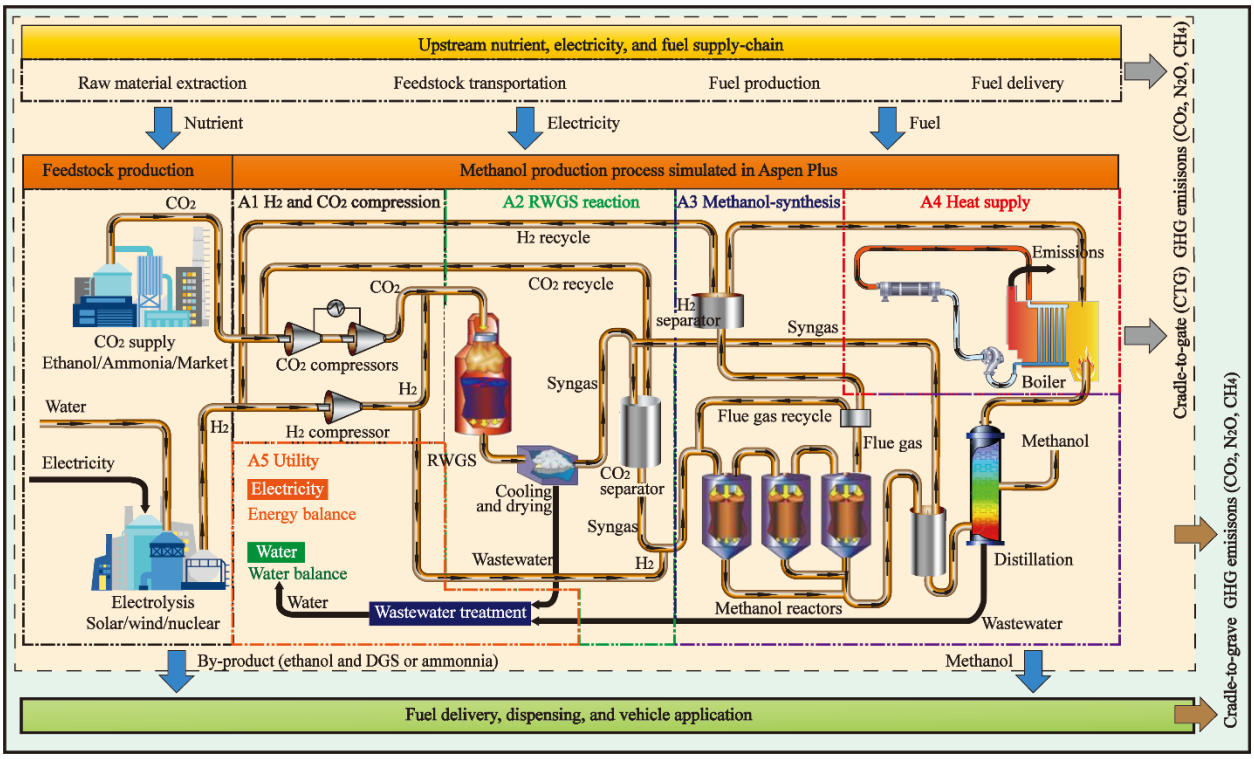

Figure 1. Process flow chart and system boundary of synthetic methanol production for CTG and cradle-to-grave life cycle analysis.

Life Cycle Analysis Methodology

Three systems are defined in this work: stand-alone methanol production system, integrated methanol-ethanol co-production system, integrated methanol-ammonia co-production system. The system boundaries defined by inputs and outputs are summarized in Table S4. For the stand-alone system, the CO_2 feedstock is not specified, and the methanol is the only system product (therefore no allocation is needed). In contrast, for the integrated co-production system, the CO_2 source is specified, and the methanol process is connected with the CO_2 supply source, e.g., corn ethanol plant or ammonia plant. For example, for the integrated methanol-ethanol co-production system, the system inputs are corn, H_2, electricity, as well as process fuels; while the system products are

methanol, ethanol, DGS, and corn oil. Given the presence of co-product other than methanol, the total GHG emissions of the integrated system are allocated to all of the co-products (methanol, ethanol, DGS, and oil) based on energy content.

Environmental impacts of CTG and cradle-to-grave GHG emissions of synthetic methanol production using various boundaries were evaluated using GREET® 2020 model.[22] The CTG life cycle accounts for material and energy input for various stages within each boundary including corn growth/transportation (including the nutrients use), and ethanol production process for ethanol plant CO_2 cases; NG recovery and processing and ammonia production process for the ammonia plant CO_2 cases; renewable H_2 production and methanol production process from H_2 and CO_2 of methanol synthesis; and various transportation activities (Figure 1). The cradle-to-grave life cycle includes all the CTG emissions plus the emissions from methanol's delivery, dispensing, and methanol consumption. The GHG emissions include CO_2, CH_4, and N_2O combined with their global warming potentials of 1, 30, and 265, respectively, using a functional unit of 1 MJ of synthesis methanol.

The energy use and GHG emissions of water electrolysis for H_2 production were obtained from GREET® 2020, assuming the H_2 transportation distance is 16 km to methanol production sites.[37] For the integrated co-production system boundary (methanol-ethanol or methanol-ammonia), the CO_2 feedstock for methanol production is supplied from the ethanol/ammonia process. A dry milling corn ethanol process with corn oil extraction and an industrial scale ammonia production process (with an amine CO_2 separation) were assumed for this study.[38,39]

The process level information for ethanol, ammonia and methanol production is provided in Table S4 of the Supporting Information. The ethanol and ammonia production utilized mass and energy

balance information in GREET®, while the methanol production information was obtained from Aspen Plus simulation as mentioned above.

For the dry milling corn ethanol process, 0.81 kg of dried distillers' grains (DGS) and 0.03 kg of oil are co-produced with 1.00 kg of ethanol. The high-purity CO_2 released from the fermentation process is from industrial data that has a 0.68 of mass ratio (CO_2: ethanol), calculated from the carbon balance by assuming that corn has a moisture content of 15%[40] and a dry base carbon content of 45%,[41] while the DGS (dry based) and corn oil have a carbon content of 49%[42] and 76%[43], respectively. The detailed mass ratio calculation processes are shown in the Supporting Information.

The theoretical conversion processes for ammonia production are listed in reaction (R4) and (R5), with detailed processes descriptions shown in the Supporting Information. Ammonia plants have onsite steam methane reforming (SMR) to produce H_2 and CO_2, which can be separated by either PSA or amine absorption. Currently, approximately 80% of the ammonia plants use amine absorption to produce high purity CO_2 with a concentration of 97.1 vol%.[9,44] Thus the resultant CO_2 is high purity (~97.1 vol%), which only needs to be compressed for feeding RWGS in the methanol production process. When the high purity CO_2 is produced from amine CO_2 separator, the mass ratio of ammonia to CO_2 is 1:1.09 according to a typical industrial ammonia production process.[45,46] More ammonia plant information is supplied in the Supporting Information.

$$0.88CH_4 + 1.26Air + 1.24H_2O \rightarrow 0.88CO_2 + N_2 + 3H_2 \quad \text{(R4)}$$

$$N_2 + 3H_2 \rightarrow 2NH_3 \quad \text{(R5)}$$

For the integrated co-production system boundary, the energy and emissions burdens are allocated to all system products. For methanol-ethanol co-production system, a hybrid allocation method

was used in which DGS and oil were treated with a marginal method (i.e., given displacement credit),[47] while methanol and ethanol shared process burden through energy (lower heating value [LHV]). Similarly, the total GHG emissions from the methanol-ammonia co-production system were allocated to methanol and ammonia based on their energy content; while for the stand-alone methanol production process, all the emissions were assigned to methanol. For the CTG and cradle-to-grave base case analysis, H_2 is produced from low-temperature electrolysis (LTE) solar/wind electrolysis (with an energy efficiency of 72%), electricity needed for the methanol production from H_2 and CO_2 is supplied by U.S. mix grid (assuming H_2 and methanol are produced from different locations), and the total emissions of the co-production systems are allocated to methanol based on energy content. By assuming the lower heating values (LHV) of methanol, ethanol, and ammonia are 26.95 MJ/kg, 18.90 MJ/kg, and 20.09 MJ/kg,[40] the energy allocation ratio of the methanol in the methanol-ethanol co-production system and methanol-ammonia system are 25.3% and 41.1%, respectively.

Besides the base case, H_2 produced from LTE nuclear electrolysis (with an energy efficiency of 72%), H_2 produced from high-temperature electrolysis (HTE) nuclear electrolysis (with an energy efficiency of 80%), and methanol produced using solar/wind renewable electricity were also studied as alternative cases. Table S4 provides the mass and energy conversion information for ethanol, ammonia, and methanol production based on GREET® and Aspen Plus models.

Cost Analysis Methodology

The H2A Production Model Framework was used for the TEA, with 2016 reference year U.S. dollar.[24] A discounted cash flow analysis was used to determine the MFSP (minimum fuel selling price) of methanol to obtain a zero net present value (NPV) in 40 operation years considering total

capital investment (TCI) and operating cost (OC), among other costs.[48] The key economic and financial assumptions are provided in Table S5 of the Supporting Information. [23]

In the TEA model, TCI is calculated according to Equation (6) using the total direct capital cost (TDCC) value. TDCC is the sum of the installed equipment costs, scaled from reference equipment cost as shown in Equation (7).[24]

$$\mathrm{TCI} = \mathrm{TDCC} + 42\% \times \mathrm{TDCC} + \$13.6/m^2 \times 40{,}469 m^2 \quad (6)$$

$$TDCC = \sum I_i \times C_{0,i} \times (S_i/S_{0,i})^{f_i} \quad (7)$$

where $TDCC$ is the total direct capital costs, I_i is the installation factor for equipment i (Table S6), $C_{0,i}$ and $S_{0,i}$ are the equipment cost and equipment size for the reference equipment scale, S_i is the designed equipment scale from Aspen Plus model, and f_i is the scaling exponent for each equipment (Table S6). The total depreciable non-equipment capital cost is $42\% \times \mathrm{TDCC}$, which includes $2\% \times \mathrm{TDCC}$ for site preparation, $10\% \times \mathrm{TDCC}$ for engineering and design, $15\% \times \mathrm{TDCC}$ for project contingency, and $15\% \times \mathrm{TDCC}$ for upfront permitting costs. The estimated land footprint cost is $\$13.6/m^2 \times 40{,}469 m^2$.

The operating cost includes fixed operating costs (FOC) and variable operating costs (VOC) using the calculation processes shown in Equation (8) and (9).

$$FOC = LC + 20\% \times LC + 2\% \times TCI + 0.3\% \times TCI \quad (8)$$

$$VOC = \sum \dot{m}_i \times C_i \quad (9)$$

In equation (8), LC is the burdened labor cost, including overhead for a labor number of 68, $20\% \times LC$ is the general and administrative expense, $2\% \times TCI$ is for the property tax and

insurance, and $0.3\% \times TCI$ is the annual maintenance and repair cost. In equation (9), $\dot{m}_i$ are the annual mass consumption of H_2 and CO_2 feedstock, industrial electricity consumption, cooling water use, process water use, and catalyst that are supplied by the Aspen Plus model, while C_i is the price of the individual inputs and materials.

For the TEA, various H_2 prices were discussed from H2A default cases, and \$2.0/kg for H_2, the Department of Energy (DOE) Hydrogen and Fuel Cell Technologies Office (HFTO) target price produced from water central electrolysis, is selected as a reference for the base case study.[49] For the three different systems of methanol-ethanol co-production, methanol-ammonia co-production, and methanol stand-alone production, the CO_2 costs are assumed to be \$17.3/MT, \$20.6/MT,[9] and \$38.6/MT,[50] respectively. The CO_2 prices of \$17.3/MT and \$20.6/MT accounts for the cost of separation, purification, and compression,[9] while the \$38.6/MT represents the traded CO_2 market price contracted by a Dakota Gasification Company.[50] The prices of process water, cooling water, and industrial electricity are assumed to be \$0.63/MT, \$0.03/MT, and \$0.07/kWh, respectively.[24] The total catalyst cost for RWGS and methanol synthesis is \$2,254K (K is thousand), replaced once every three years.[51]

RESULTS

Processes Modeling Results

The modeled process produces 1,190 MT/day methanol by consuming 243 MT/day H_2 and 1,978 MT/day CO_2 (with a molar ratio of 2.7:1.0) (Table S2 and Figure S1 in Supporting Information). When this CO_2 is supplied by the ethanol plant or ammonia plant, the integrated system produces 2,912 MT/day of ethanol, 2,369 MT/day of DGS, and 83 MT/day of corn oil; or 1,817 MT/day of ammonia (Table 1).

Table 1 shows that the methanol production efficiency is 75.6%, considering the total process energy input, i.e., including both H_2 and electricity . Whereas for the stand-alone methanol production system, the CTG methanol production efficiency is 51.8%, considering the CTG total energy input, i.e., including the upstream energy use for H_2 production . When the methanol production process is integrated with the ethanol or ammonia production process, the methanol CTG energy efficiency is 62.5% and 48.3%, respectively. The detailed material consumptions and CTG energy consumption for methanol, ethanol, and ammonia stand-alone production processes are shown in Table S3 and Table S4.

In the methanol production process, 82.5% of carbon in CO_2 feedstock is converted into methanol with the detailed carbon balance shown in Figure 2. In Figure 2, for the stand-alone methanol system, 82.5% of carbon from CO_2 feedstock (1,872 kmol/hr) is converted into methanol (1,545 kmol/hr), with 17.0% carbon emitted from combustion of tail gas in boiler, and the other 0.5% carbon emitted from CO_2 capture unit. For the methanol-ethanol co-production system, the carbon in corn is the carbon source for the total system; in the ethanol production process, 46.3%, 35.3%, and 1.9% of carbon in corn have been converted into ethanol, DGS, and oil, while the 16.5% remaining carbon is released as high-purity CO_2, which is used for methanol production. The total carbon conversion ratio of the methanol-ethanol co-production system is 97.1%; that is 13.6% higher than that of the corn ethanol (stand-alone) plant. For the methanol-ammonia co-production system, natural gas (NG) is the carbon source. In the ammonia production process, 53.0% of the NG carbon is produced as high-purity CO_2, which is used for methanol production, resulting in a total carbon conversion ratio of 43.8% for the methanol-ammonia co-production system.

Table 1. Performance analysis results of the three systems.

	Methanol production system	Methanol-ethanol co-production system	Methanol-ammonia co-production system
H_2 consumption (MT/day) [a]	243	243	243
High purity CO_2 consumption (MT/day) [a]	1,978	0	0
Ethanol production (MT/day) [b]	0	2,912	0
Ammonia production (MT/day) [c]	0	0	1,817
DGS production (MT/day) [b]	0	2,369	0
Corn oil production (MT/day) [b]	0	83	0
Methanol production (MT/day) [a]	1,190	1,190	1,190
Total carbon conversion efficiency (%) [a]	82.5%	82.5%	82.5%
H_2 input for methanol synthesis (MW) [a]	337.8	337.8	337.8
Electric power input for methanol synthesis (MW) [a]	28.0	28.0	28.0
CTG renewable input (MW) [d]	485.1	2327.6	489.8
CTG fossil input (MW) [d]	49.4	514.9	905.4
Ethanol (MW) [b]	0.0	908.4	0.0
Ammonia (MW) [c]	0.0	0.0	397.4
DGS (MW) [b]	0.0	555.1	0.0
Corn oil (MW) [b]	0.0	35.8	0.0
Methanol (MW) [d]	276.7	276.7	276.7
Methanol synthesis energy efficiency (%) [a]	75.6%	75.6%	75.6%
CTG methanol production efficiency (%) [d]	51.8%	9.7%	19.8%
CTG total energy efficiency (%) [d]	51.8%	62.5%	48.3%

[a] Data is from the Aspen model of methanol produced from H_2 and CO_2.
[b] Data is from the methanol-ethanol co-production system.
[c] Data is from the methanol-ammonia co-production system.
[d] Data is from the CTG energy analysis including upstream fuel and nutrient supply chain.

The result of methanol synthesis modeling is also compared with previous studies. For example, the work of Anicic et.al showed the two-step methanol synthesis process has a cold gas efficiency of 80.1% and a carbon conversion ratio of 79.0%.[14] It is worth noting that the cold gas efficiency is defined as the ratio of the energy in methanol product divided by energy in H_2 feedstock without accounting for the electricity consumption (shown in equation (2)). To allow comparison on a consistent basis, the present study also calculated the cold gas energy efficiency, without accounting for electricity consumption leading to a higher efficiency of 81.9% and a higher carbon

conversion ratio of 82.5%. The small differences in cold gas efficiency and carbon conversion ratio between this study and Anicic et.al are attributed to the different design parameters for the RWGS and methanol synthesis processes, such as reaction temperature, pressure, conversion ratio, and hydrogen recycle ratio.

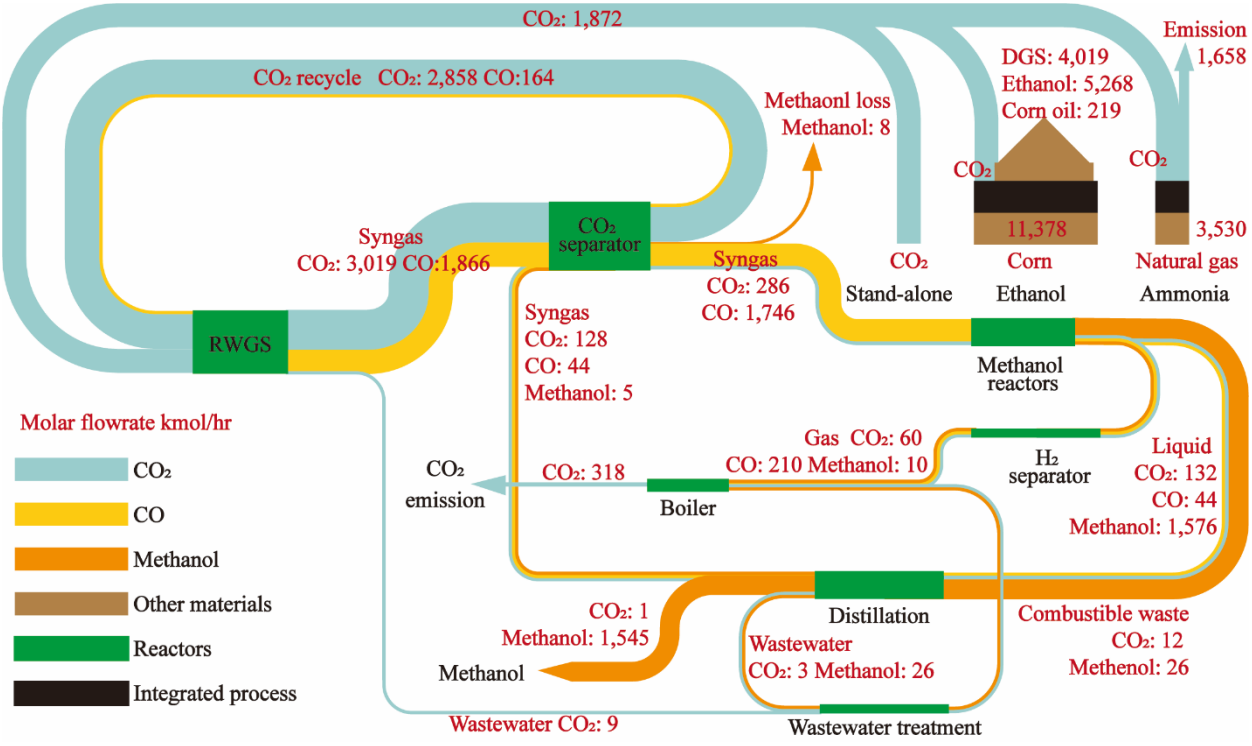

Figure 2. Sankey diagram of the carbon balance of three systems. All the values are in the unit of kmol/hr. The width of flow expresses the quantity of carbon molar flowrate in different components, the green, and black boxes represent conversion processes and integrated process, and the blue, yellow, orange, brown flows represent CO_2, CO, methanol, and other material flows, respectively.

Life Cycle Analysis Results

The CTG GHG emissions of the three considered methanol production systems were estimated with various H_2 production and electricity generation technologies, and coproduct allocation methods, as shown in Figure 3. The base case study uses H_2 production from low-temperature electrolysis (LTE) of water using wind/solar power, and energy allocation (with marginal method approach for DGS and oil from ethanol-methanol co-production system). The CTG GHG

emissions (without methanol combustion CO_2 emissions) of the stand-alone methanol production in the base case is -55.7 g CO_2-eq./MJ methanol with -68.4 g CO_2-eq./MJ from captured CO_2 embedded in methanol (blue bars in Figure 3) and 12.7 g CO_2-eq./MJ emitted, mostly from the upstream grid electricity used for methanol synthesis process.[22] When the methanol production process is integrated with the ethanol plant or ammonia plant, the total system burdens are shared or allocated by energy to both methanol and ethanol/ammonia, thus mitigating the burden on ethanol/ammonia while increasing the methanol CTG GHG emissions to -32.2 g CO_2-eq./MJ and 14.2 g CO_2-eq./MJ for the methanol-ethanol and methanol-ammonia co-production systems, respectively.

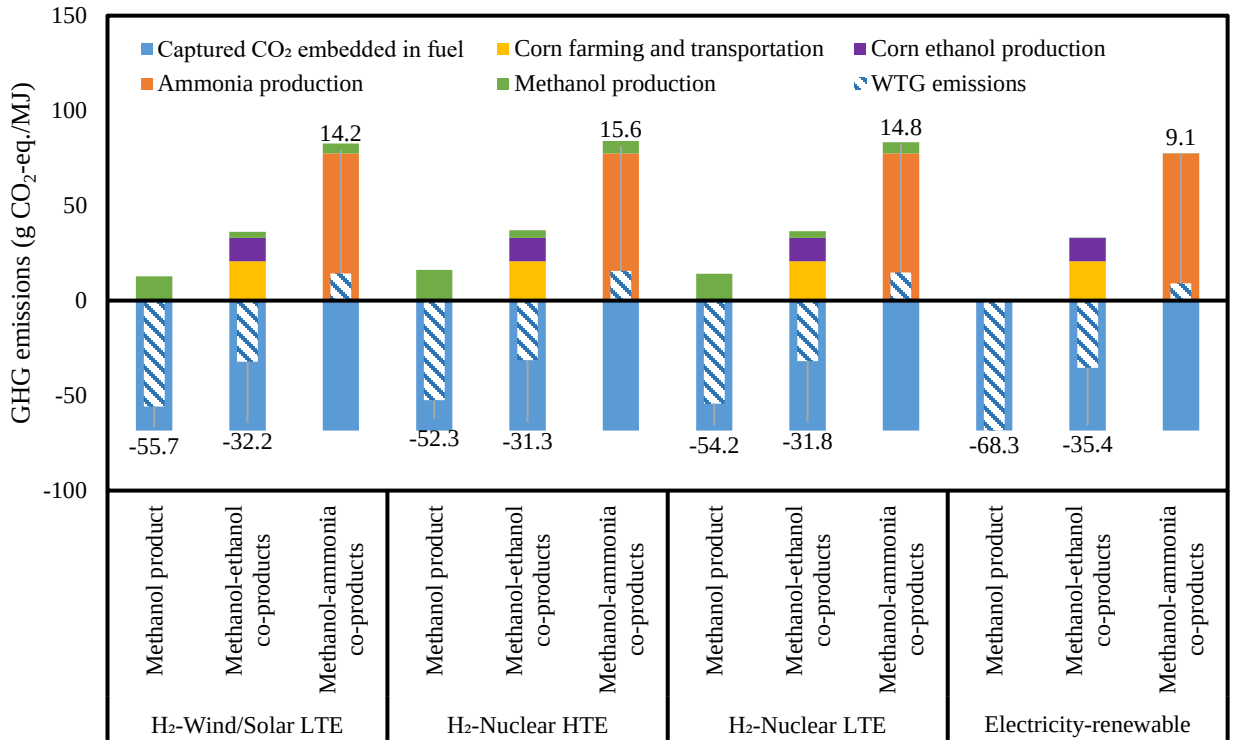

Figure 3. Methanol CTG GHG emissions with various H_2 sources, electricity types, and allocation methods. Methanol is the single product from the methanol production system, while emissions from the (integrated) co-production systems are allocated to ethanol and methanol or ammonia and methanol. The base cases use wind/solar H_2, U.S. average grid mix electricity, and energy allocation (LHV).

In addition to the H_2 produced from wind/solar LTE, two nuclear energy base H_2 production pathways of high-temperature electrolysis (HTE) and LTE were also studied. In general, the GHG emissions from nuclear HTE-H_2 pathways are 0.5–1.9 g CO_2-eq./MJ lower compared to LTE-H_2 pathways, but are 0.4–1.5 g CO_2-eq./MJ higher compared to wind/solar-H_2 pathway. When the U.S. average grid mix electricity is replaced by renewable electricity, the CTG GHG emissions of the stand-alone methanol production system are reduced to -68.3 g CO_2-eq./MJ, and that of the methanol-ethanol and methanol-ammonia co-production systems decrease by 3.2 g CO_2-eq./MJ and 5.1 g CO_2-eq./MJ, respectively.

The cradle-to-grave GHG emissions of synthetic methanol from the three aforementioned production systems are compared with the emissions from other fuels, as shown in Figure 4. Methanol from the stand-alone system with renewable electricity supply has the lowest cradle-to-grave GHG emissions of 2.0 g CO_2-eq./MJ as compared to 91.5 g CO_2-eq./MJ for the conventional methanol production from NG (i.e., 89.5 g CO_2-eq./MJ cradle-to-grave GHG emissions reduction). Using U.S. average grid electricity for methanol synthesis process, the stand-alone system has the potential to reduce cradle-to-grave GHG emissions by 74.3–77.9 g CO_2-eq./MJ with various renewable and nuclear hydrogen sources, compared to the NG-methanol pathway. When the methanol production process is integrated with the corn ethanol plant (methanol-ethanol co-production system), the cradle-to-grave GHG emissions of methanol are 52.7–56.5 g CO_2-eq./MJ lower compared to the NG-methanol pathway. The cradle-to-grave GHG emissions of methanol, considering the integrated methanol-ammonia co-production system with various electricity sources and hydrogen sources, are 5.5–12.1 g CO_2-eq./MJ lower compared to the NG-methanol pathway.

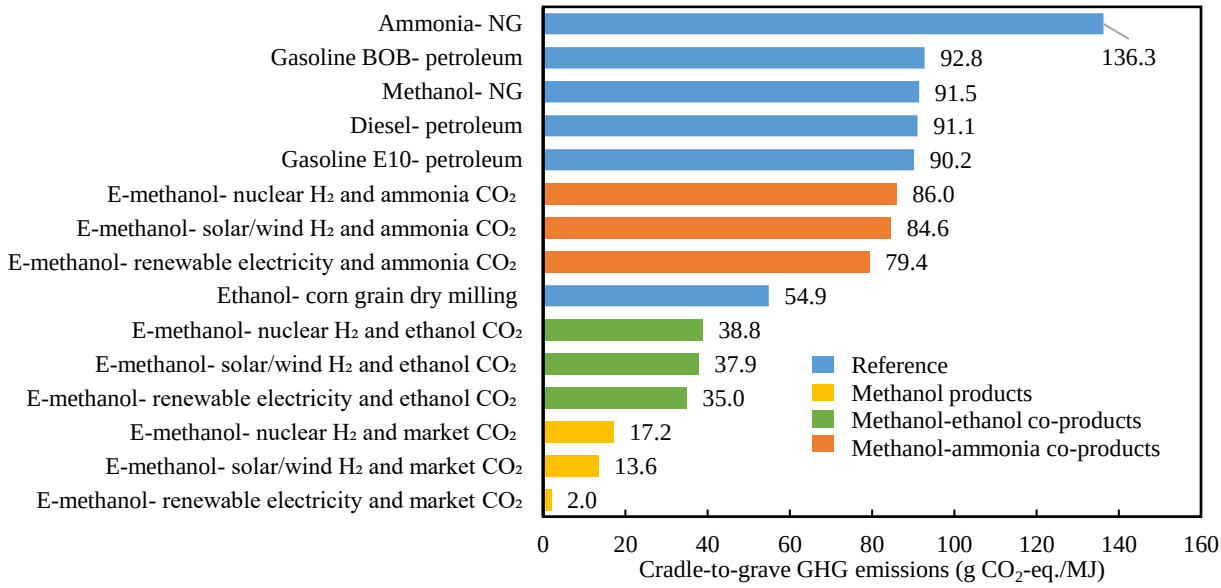

Figure 4. Cradle-to-grave GHG emissions of synthetic methanol compared with other chemicals and fuels. The blue bars are GHG emissions of conventional chemicals and petroleum fuel pathways from GREET®, the yellow bars are the GHG emissions of synthetic methanol from stand-alone production system, while the green and orange bars are the GHG emissions of methanol from the methanol-ethanol and methanol-ammonia co-production systems, respectively. BOB is short for blendstock for oxygenate blending. The cases use wind/solar LTE for H_2 production and U.S. average electricity grid mix for methanol synthesis process, and energy allocation if the details are not otherwise mentioned.

Economic Analysis Results

In this study, the CO_2 prices are assumed to be \$17.3/MT, \$20.6/MT, and \$38.6/MT for the methanol-ethanol co-production system, methanol-ammonia co-production system, and the stand-alone methanol production system, respectively. The total capital investment of the stand-alone methanol production is \$305 million (MM), with a total direct capital cost of \$213 MM (details are provided in Tables S7 and S6 of Supporting Information). For the methanol production process, the RWGS reaction area, methanol-synthesis area, and utility area have the largest installed equipment cost of \$76 MM, \$50 MM, and \$40 MM, that are 35.8%, 23.3%, and 19.0% of the total depreciable capital cost, respectively. The total variable operating cost is \$190 MM/year when the H_2 price is \$2.0/kg and CO_2 price is \$17.3/MT (Table S8). While the total fixed operating cost is

368 $17 MM/year with a labor number of 68 and a burdened labor cost including overhead of
369 $58/man-hr (Table S7).

370 Figure 5 shows the MFSP of synthetic methanol as compared to the average methanol market price
371 over the past five years of $0.38/kg. When the DOE target hydrogen production price of $2.0/kg
372 is assumed, the MFSP of the methanol from the stand-alone system is $0.64/kg, and from the co-
373 production systems (methanol-ethanol and methanol-ammonia) is $0.61/kg. The evaluated MFSPs
374 are 17–23% higher than the maximum methanol price in the past five years, and 61–68%, 144–
375 156% higher than the average and minimum methanol prices in the past five years. As shown in
376 Figure 5 for the methanol-ethanol co-production system, feedstock costs for H_2 ($2.0/kg) and CO_2
377 ($17.3/MT), and the capital costs dominate the methanol MFSP, contributing 68.9%, 4.8%, and
378 10.5%, respectively. When H_2 is produced from renewable electricity using the current renewable
379 polymer electrolyte membrane electrolysis (PEME) technology, the H_2 price increases to
380 $5.0/kg,[49] resulting in a higher MFSP of methanol ($1.24–1.28/kg). However, given that the low
381 cradle-to-grave GHG emission of the stand-alone methanol production system is 2.0–17.2 g CO_2-
382 eq./MJ, the synthetic methanol production using renewable hydrogen can be qualified as a low-
383 carbon fuel compared to conventional methanol production from NG (with a cradle-to-grave GHG
384 emissions of 91.5 g CO_2-eq./MJ). If avoided CO_2 can be traded in a carbon trading market, the
385 potential carbon credit can further reduce the MFSP of synthetic methanol, as shown in Figure 5.
386 According to the Section 45Q carbon capture tax credit, the CO_2 utilization for synthetic methanol
387 production has a CO_2 credit of $35/MT.[52] With a CO_2 credit of $35/MT, the synthetic methanol
388 MFSP is $0.56–0.59/kg, which is $0.05/MT lower than the cases with zero CO_2 credit. If the CO_2
389 credit increases to $200/MT,[53] the synthetic methanol MFSP from the stand-alone production
390 system is $0.18/kg, and from the methanol-ethanol and methanol-ammonia co-production systems

is $0.15/kg, which are 52.6% and 60.5% lower than the average methanol market price in the past five years. Given that the variation of the TEA assumptions results in uncertainty of the MFSP, MFSP cost distributions, sensitivity analysis, and uncertainty analysis results are supplied in the Supporting Information Figure S4-S6.

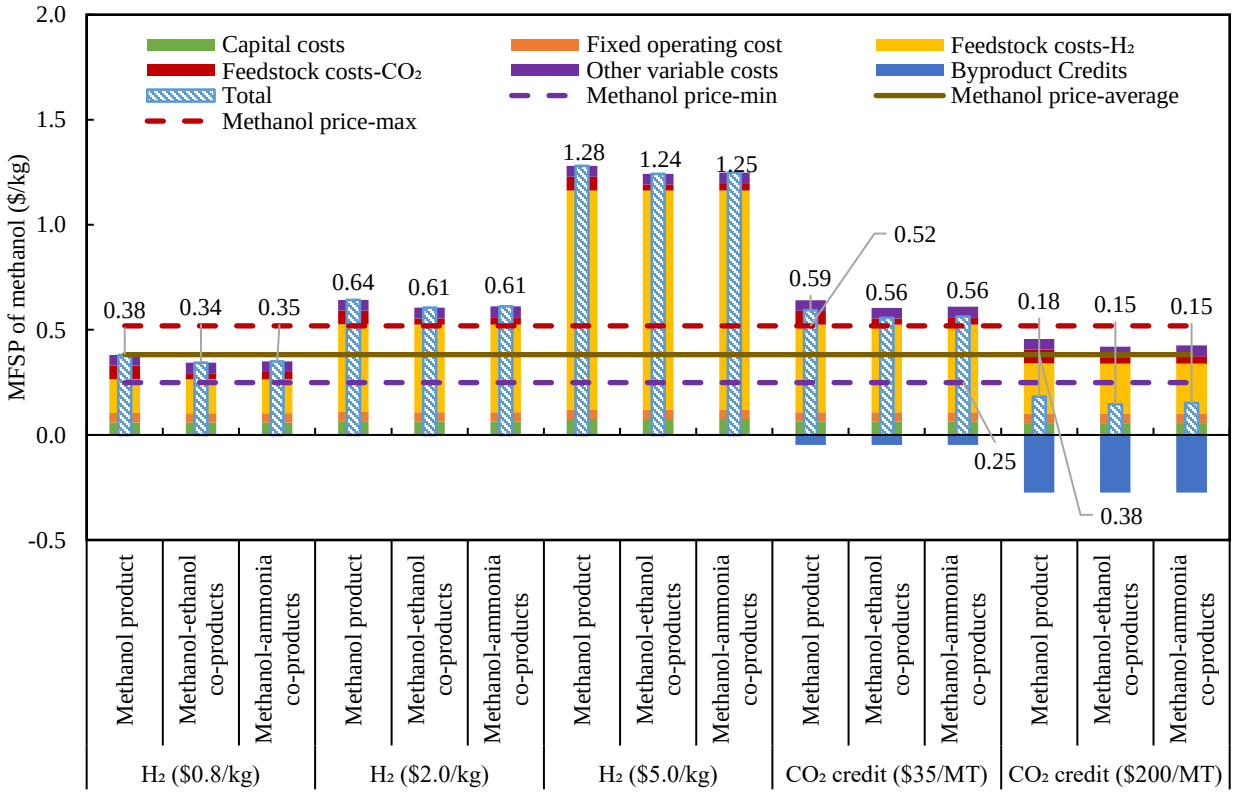

Figure 5. Variation of MFSP with H_2 price and potential CO_2 credit.

Figure 6 shows the breakeven H_2 prices for the MFSP of methanol to equal the average methanol market price ($0.38/kg) for different methanol production system boundaries and various CO_2 credit values. For the cases without CO_2 credit, the breakeven H_2 prices for the three evaluated systems are within $0.77–0.95/kg. However, for the cases with $200/MT CO_2 credit, the breakeven H_2 prices are $2.09–2.24/kg. The TEA results indicate that the economics of synthetic methanol production can be improved by developing low-cost water electrolysis technology for renewable H_2 production and leveraging credits in carbon trading markets.

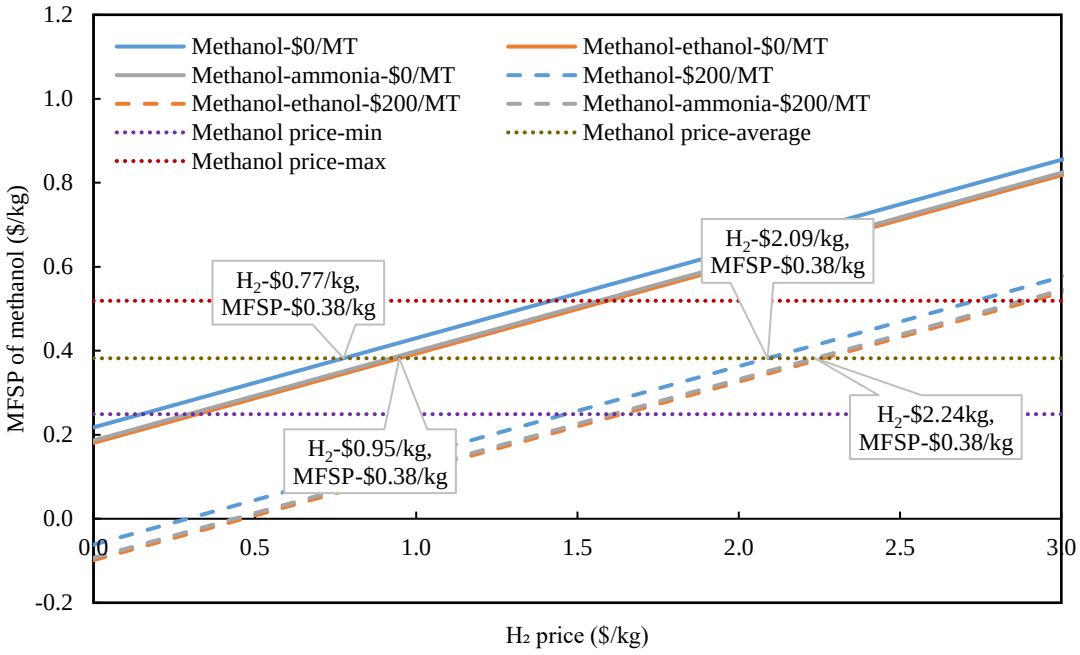

Figure 6. Breakeven H_2 prices for different methanol production systems and various CO_2 credit values. In the legend, \$0/MT refers to CO_2 credit of \$0/MT, and \$200/MT refers to CO_2 credit of \$200/MT. The call-out shows the breakeven H_2 price such that the MFSP of methanol equals the average methanol market price of \$0.38/kg.

IMPLICATIONS

The present study evaluated TEA and LCA of synthetic methanol using high purity CO_2 from ethanol and ammonia plants, with various price scenarios. Simulation results show that integrating methanol synthesis with ethanol and ammonia production improves the production energy efficiency, carbon conversion efficiency, and GHG emissions.

This study used high purity CO_2 emissions from typical ethanol and ammonia plants as feedstock for the synthetic methanol production. The integrated system boundary treatment can be extended to other industries such as cement, iron and steel, carbonates, and petrochemicals. Moreover, if the current results are scaled to combine with the industrial distribution data of the ethanol and ammonia plants in the U.S., the potential total H_2 market demand and the potential total synthetic methanol production, as well as their environmental impacts can be further evaluated.

SUPPORTING INFORMATION

Additional details on simulation assumptions, flow results, mass and energy balance of methanol production from H_2 and CO_2; system boundary of stand-alone and integrated systems; ethanol production processes; ammonia production processes; techno-economic analysis assumptions and cost results; methanol MFSP components, sensitivity analysis and risk analysis of MFSP of methanol.

ACKNOWLEDGMENTS

This research was supported by the Hydrogen and Fuel Cell Technologies Office (HFTO) of the U.S. Department of Energy's Office of Energy Efficiency and Renewable Energy under Contract No. DE-AC02-06CH11357. The authors are grateful to the support and guidance of Dr. Sunita Satyapal and Neha Rustagi from HFTO.

LIST OF ABBREVIATIONS

BOB	Blendstock for oxygenate blending
CO_2	Carbon dioxide
CCU	Carbon capture and utilization
DCFROR	Discounted cash flow rate of return
DOE	Department of Energy
E-fuels	Electro-fuels
FOC	Fixed operating costs
GHG	Greenhouse gas
GREET	Greenhouse gases, Regulated Emissions and Energy use in Transportation
H_2	Hydrogen
HFTO	Hydrogen and Fuel Cell Technologies Office
LCA	Life cycle analysis
LHV	Lower heating value
LTE	Low-temperature electrolysis
MFSP	Minimum fuel selling price
NG	Natural gas

NPV	Net present value
OC	Operating cost
PEME	Polymer electrolyte membrane electrolysis
PSA	Pressure swing adsorption
RWGS	Reverse water gas shift
SMR	Steam methane reforming
SOEC	Solid oxide electrolyzer cell
TCI	Total capital investment
TDCC	Total direct capital cost
TEA	Techno-economic analysis
THE	High-temperature electrolysis
VOC	Variable operating costs
CTG	Cradle-to-gate

REFERENCES

(1) Hockstad, L.; Hanel, L. *Inventory of US Greenhouse Gas Emissions and Sinks*; Environmental System Science Data Infrastructure for a Virtual Ecosystem, 2018.

(2) Yeh, S.; Lutsey, N. P.; Parker, N. C. Assessment of Technologies to Meet a Low Carbon Fuel Standard. *Environ. Sci. Technol.* **2009**, *43* (18), 6907–6914. https://doi.org/10.1021/es900262w.

(3) Venkatesh, A.; Jaramillo, P.; Griffin, W. M.; Matthews, H. S. Uncertainty Analysis of Life Cycle Greenhouse Gas Emissions from Petroleum-Based Fuels and Impacts on Low Carbon Fuel Policies. *Environ. Sci. Technol.* **2011**, *45* (1), 125–131. https://doi.org/10.1021/es102498a.

(4) von der Assen, N.; Müller, L. J.; Steingrube, A.; Voll, P.; Bardow, A. Selecting CO2 Sources for CO2 Utilization by Environmental-Merit-Order Curves. *Environ. Sci. Technol.* **2016**, *50* (3), 1093–1101. https://doi.org/10.1021/acs.est.5b03474.

(5) Anwar, M. N.; Fayyaz, A.; Sohail, N. F.; Khokhar, M. F.; Baqar, M.; Yasar, A.; Rasool, K.; Nazir, A.; Raja, M. U. F.; Rehan, M.; Aghbashlo, M.; Tabatabaei, M.; Nizami, A. S. CO2 Utilization: Turning Greenhouse Gas into Fuels and Valuable Products. *J. Environ. Manage.* **2020**, *260*, 110059. https://doi.org/https://doi.org/10.1016/j.jenvman.2019.110059.

(6) Fernández-Dacosta, C.; Shen, L.; Schakel, W.; Ramirez, A.; Kramer, G. J. Potential and Challenges of Low-Carbon Energy Options: Comparative Assessment of Alternative Fuels for the Transport Sector. *Appl. Energy* **2019**, *236*, 590–606. https://doi.org/https://doi.org/10.1016/j.apenergy.2018.11.055.

(7) Supekar, S. D.; Skerlos, S. J. Market-Driven Emissions from Recovery of Carbon Dioxide Gas. *Environ. Sci. Technol.* **2014**, *48* (24), 14615–14623. https://doi.org/10.1021/es503485z.

(8) Bains, P.; Psarras, P.; Wilcox, J. CO2 Capture from the Industry Sector. *Prog. Energy Combust. Sci.* **2017**, *63*, 146–172. https://doi.org/https://doi.org/10.1016/j.pecs.2017.07.001.

(9) Herron, S.; Zoelle, A.; Summers, W. M. *Cost of Capturing CO2 from Industrial Sources*; NETL, 2014.

(10) Greenhouse Gas Reporting Program (GHGRP). *Greenhouse Gas Reporting Program Industrial*

Profile: Chemicals Sector; Washington, DC, 2019.

(11) Irlam, L.; Policy, S. A.; Economics, A.-P. R. Global Costs of Carbon Capture and Storage. *Glob. CCS Institute, Melbourne, Aust.* **2017**.

(12) He, Z.; Cui, M.; Qian, Q.; Zhang, J.; Liu, H.; Han, B. Synthesis of Liquid Fuel via Direct Hydrogenation of CO₂ *Proc. Natl. Acad. Sci.* **2019**, *116* (26), 12654 LP – 12659. https://doi.org/10.1073/pnas.1821231116.

(13) Pérez-Fortes, M.; Schöneberger, J. C.; Boulamanti, A.; Tzimas, E. Methanol Synthesis Using Captured CO2 as Raw Material: Techno-Economic and Environmental Assessment. *Appl. Energy* **2016**, *161*, 718–732. https://doi.org/https://doi.org/10.1016/j.apenergy.2015.07.067.

(14) Anicic, B.; Trop, P.; Goricanec, D. Comparison between Two Methods of Methanol Production from Carbon Dioxide. *Energy* **2014**, *77*, 279–289. https://doi.org/https://doi.org/10.1016/j.energy.2014.09.069.

(15) Kim, J.; Henao, C. A.; Johnson, T. A.; Dedrick, D. E.; Miller, J. E.; Stechel, E. B.; Maravelias, C. T. Methanol Production from CO2 Using Solar-Thermal Energy: Process Development and Techno-Economic Analysis. *Energy Environ. Sci.* **2011**, *4* (9), 3122–3132.

(16) Artz, J.; Müller, T. E.; Thenert, K.; Kleinekorte, J.; Meys, R.; Sternberg, A.; Bardow, A.; Leitner, W. Sustainable Conversion of Carbon Dioxide: An Integrated Review of Catalysis and Life Cycle Assessment. *Chem. Rev.* **2018**, *118* (2), 434–504. https://doi.org/10.1021/acs.chemrev.7b00435.

(17) Michailos, S.; Sanderson, P.; Villa Zaragoza, A.; McCord, S.; Armstrong, K.; Styring, P.; Mason, F.; Stokes, G.; Williams, E.; Zimmermann, A. Methanol Worked Examples for the TEA and LCA Guidelines for CO2 Utilization. **2018**.

(18) Pérez-Fortes, M.; Tzimas, E. Techno-Economic and Environmental Evaluation of CO2 Utilisation for Fuel Production. *JRC Sci. Hub ZG Petten, Netherlands* **2016**.

(19) Hank, C.; Gelpke, S.; Schnabl, A.; White, R. J.; Full, J.; Wiebe, N.; Smolinka, T.; Schaadt, A.; Henning, H.-M.; Hebling, C. Economics & Carbon Dioxide Avoidance Cost of Methanol Production Based on Renewable Hydrogen and Recycled Carbon Dioxide–Power-to-Methanol. *Sustain. Energy Fuels* **2018**, *2* (6), 1244–1261.

(20) Szima, S.; Cormos, C.-C. Improving Methanol Synthesis from Carbon-Free H2 and Captured CO2: A Techno-Economic and Environmental Evaluation. *J. CO2 Util.* **2018**, *24*, 555–563. https://doi.org/https://doi.org/10.1016/j.jcou.2018.02.007.

(21) Biernacki, P.; Röther, T.; Paul, W.; Werner, P.; Steinigeweg, S. Environmental Impact of the Excess Electricity Conversion into Methanol. *J. Clean. Prod.* **2018**, *191*, 87–98. https://doi.org/https://doi.org/10.1016/j.jclepro.2018.04.232.

(22) Wang, M.; Elgowainy, Amgad; Pahola, Michael Wang, Amgad Elgowainy, U. L.; Pahola Thathiana Benavides, Andrew Burnham, Hao Cai, Qiang Dai, T. R. H.; Jarod Cory Kelly, Hoyoung Kwon, Xinyu Liu, Zifeng Lu, Longwen Ou, Pingping Sun, Olumide Winjobi, H. X. *Summary of Expansions and Updates in GREET® 2019*; United States, 2019. https://doi.org/10.2172/1483843.

(23) Zang, G.; Sun, P.; Elgowainy, A. A.; Bafana, A.; Wang, M. Performance and Cost Analysis of Liquid Fuel Production from H2 and CO2 Based on the Fischer-Tropsch Process. *J. CO2 Util.* **2021**, *46*, 101459. https://doi.org/https://doi.org/10.1016/j.jcou.2021.101459.

(24) Penev Golden, CO (United States)] (ORCID:0000000283021565), M. [National R. E. L. (NREL).

Techno-Economic Modelling with H2A and H2FAST; United States, 2020.

(25) Saeidi, S.; Najari, S.; Fazlollahi, F.; Nikoo, M. K.; Sefidkon, F.; Klemeš, J. J.; Baxter, L. L. Mechanisms and Kinetics of CO2 Hydrogenation to Value-Added Products: A Detailed Review on Current Status and Future Trends. *Renew. Sustain. Energy Rev.* **2017**, *80*, 1292–1311. https://doi.org/https://doi.org/10.1016/j.rser.2017.05.204.

(26) Al-Kalbani, H.; Xuan, J.; García, S.; Wang, H. Comparative Energetic Assessment of Methanol Production from CO2: Chemical versus Electrochemical Process. *Appl. Energy* **2016**, *165*, 1–13. https://doi.org/https://doi.org/10.1016/j.apenergy.2015.12.027.

(27) Lee, D.-Y.; Elgowainy, A. By-Product Hydrogen from Steam Cracking of Natural Gas Liquids (NGLs): Potential for Large-Scale Hydrogen Fuel Production, Life-Cycle Air Emissions Reduction, and Economic Benefit. *Int. J. Hydrogen Energy* **2018**, *43* (43), 20143–20160. https://doi.org/https://doi.org/10.1016/j.ijhydene.2018.09.039.

(28) Humbird, D.; Davis, R.; Tao, L.; Kinchin, C.; Hsu, D.; Aden, A.; Schoen, P.; Lukas, J.; Olthof, B.; Worley, M. *Process Design and Economics for Biochemical Conversion of Lignocellulosic Biomass to Ethanol: Dilute-Acid Pretreatment and Enzymatic Hydrolysis of Corn Stover*; National Renewable Energy Lab.(NREL), Golden, CO (United States), 2011.

(29) Kim, D. H.; Park, J. L.; Park, E. J.; Kim, Y. D.; Uhm, S. Dopant Effect of Barium Zirconate-Based Perovskite-Type Catalysts for the Intermediate-Temperature Reverse Water Gas Shift Reaction. *ACS Catal.* **2014**, *4* (9), 3117–3122. https://doi.org/10.1021/cs500476e.

(30) Zang, G.; Zhang, J.; Jia, J.; Lora, E. S.; Ratner, A. Life Cycle Assessment of Power-Generation Systems Based on Biomass Integrated Gasification Combined Cycles. *Renew. Energy* **2020**, *149*, 336–346. https://doi.org/https://doi.org/10.1016/j.renene.2019.12.013.

(31) Phillips, S. D.; Tarud, J. K.; Biddy, M. J.; Dutta, A. *Gasoline from Wood via Integrated Gasification, Synthesis, and Methanol-to-Gasoline Technologies*; United States, 2011. https://doi.org/10.2172/1004790.

(32) Spath, P.; Aden, A.; Eggeman, T.; Ringer, M.; Wallace, B.; Jechura, J. *Biomass to Hydrogen Production Detailed Design and Economics Utilizing the Battelle Columbus Laboratory Indirectly-Heated Gasifier*; United States, 2005. https://doi.org/10.2172/15016221.

(33) Zang, G.; Tejasvi, S.; Ratner, A.; Lora, E. S. A Comparative Study of Biomass Integrated Gasification Combined Cycle Power Systems: Performance Analysis. *Bioresour. Technol.* **2018**, *255*, 246–256. https://doi.org/https://doi.org/10.1016/j.biortech.2018.01.093.

(34) Davis, R.; Tao, L.; Tan, E. C. D.; Biddy, M. J.; Beckham, G. T.; Scarlata, C.; Jacobson, J.; Cafferty, K.; Ross, J.; Lukas, J.; Knorr, D.; Schoen, P. *Process Design and Economics for the Conversion of Lignocellulosic Biomass to Hydrocarbons: Dilute-Acid and Enzymatic Deconstruction of Biomass to Sugars and Biological Conversion of Sugars to Hydrocarbons*; United States, 2013. https://doi.org/10.2172/1107470.

(35) Gong, M.; Yi, Q.; Huang, Y.; Wu, G.; Hao, Y.; Feng, J.; Li, W. Coke Oven Gas to Methanol Process Integrated with CO2 Recycle for High Energy Efficiency, Economic Benefits and Low Emissions. *Energy Convers. Manag.* **2017**, *133*, 318–331. https://doi.org/https://doi.org/10.1016/j.enconman.2016.12.010.

(36) Kuo, P.-C.; Wu, W. Thermodynamic Analysis of a Combined Heat and Power System with CO2 Utilization Based on Co-Gasification of Biomass and Coal. *Chem. Eng. Sci.* **2016**, *142*, 201–214. https://doi.org/https://doi.org/10.1016/j.ces.2015.11.030.

(37) Saadi, F. H.; Lewis, N. S.; McFarland, E. W. Relative Costs of Transporting Electrical and Chemical Energy. *Energy Environ. Sci.* **2018**, *11* (3), 469–475. https://doi.org/10.1039/C7EE01987D.

(38) Wang, Zhichao ; Dunn, Jennifer B. ; Wang, M. Q. *Updates to the Corn Ethanol Pathway and Development of an Integrated Corn and Corn Stover Ethanol Pathway in the GREET™ Model*; United States, 2014. https://doi.org/10.2172/1172034.

(39) Aspen Technology. *Aspen Plus Ammonia Model*; Bedford, MA, 2015.

(40) Wang, M.; Elgowainy, A.; Lee, U.; Bafana, A.; Benavides, P. T.; Bumham, A.; Cai, H.; Dai, Q. *Summary of Expansions and Updates in GREET® 2020*; Lemont, IL, US, 2020.

(41) Latshaw, W. L.; Miller, E. C. Elemental Composition of the Corn Plant. *J. Agric. Res.* **1924**, *27* (11), 845–861.

(42) Giuntoli, J.; de Jong, W.; Arvelakis, S.; Spliethoff, H.; Verkooijen, A. H. M. Quantitative and Kinetic TG-FTIR Study of Biomass Residue Pyrolysis: Dry Distiller's Grains with Solubles (DDGS) and Chicken Manure. *J. Anal. Appl. Pyrolysis* **2009**, *85* (1), 301–312. https://doi.org/https://doi.org/10.1016/j.jaap.2008.12.007.

(43) Nagaraja, S.; Soorya Prakash, K.; Sudhakaran, R.; Sathish Kumar, M. Investigation on the Emission Quality, Performance and Combustion Characteristics of the Compression Ignition Engine Fueled with Environmental Friendly Corn Oil Methyl Ester – Diesel Blends. *Ecotoxicol. Environ. Saf.* **2016**, *134*, 455–461. https://doi.org/https://doi.org/10.1016/j.ecoenv.2016.01.023.

(44) Unite States Enviromental Protection Agency (EPA). *Emissions Facts: Ammonia Synthesis*.

(45) Association, E. F. M. Best Available Techniques for Pollution Prevention and Control in the European Fertilizer Industry. *Prod. Urea Urea Ammonium Nitrate* **2000**.

(46) Kheshgi, H. S.; Prince, R. C. Sequestration of Fermentation CO2 from Ethanol Production. *Energy* **2005**, *30* (10), 1865–1871. https://doi.org/https://doi.org/10.1016/j.energy.2004.11.004.

(47) Rosenfeld, J.; Lewandrowski, J.; Hendrickson, T.; Jaglo, K.; Moffroid, K.; Pape, D. *A Life-Cycle Analysis of the Greenhouse Gas Emissions from Corn-Based Ethanol*; Washington, DC, 2018. https://doi.org/Report prepared by ICF under USDA Contract No. AG-3142-D-17-0161.

(48) Zang, G.; Shah, A.; Wan, C. Techno-Economic Analysis of an Integrated Biorefinery Strategy Based on One-Pot Biomass Fractionation and Furfural Production. *J. Clean. Prod.* **2020**, *260*, 120837. https://doi.org/https://doi.org/10.1016/j.jclepro.2020.120837.

(49) Peterson, David; Vickers, James; Desantis, D. *DOE Hydrogen and Fuel Cells Program Record: Hydrogen Production Cost from PEM Electrolysis*; 2019.

(50) Energy, D. *Commercial CO2 Market Today. Efficiently Producing Fuels from Waste CO2 and off-Peak Wind*; 2011.

(51) Swanson, R. M.; Platon, A.; Satrio, J. A.; Brown, R. C.; Hsu, D. D. *Techno-Economic Analysis of Biofuels Production Based on Gasification*; United States, 2010. https://doi.org/10.2172/994017.

(52) Christensen, J. Primer: Section 45Q Tax Credit for Carbon Capture Projects https://www.betterenergy.org/blog/primer-section-45q-tax-credit-for-carbon-capture-projects/. https://doi.org/https://www.betterenergy.org/blog/primer-section-45q-tax-credit-for-carbon-capture-projects/.

(53) Hu, K.; Chen, Y. Equilibrium Fuel Supply and Carbon Credit Pricing under Market Competition

584 and Environmental Regulations: A California Case Study. *Appl. Energy* **2019**, *236*, 815–824.
585 https://doi.org/https://doi.org/10.1016/j.apenergy.2018.12.041.

586